Supplementary Information

Materials and Methods

Supplementary Figures 1-10

Supplementary Tables 1-10

Materials and Methods

Chromatin immunoprecipitation

Chromatin immunoprecipitation (ChIP) was performed as previously described (Massie et al, 2007; Schmidt et al, 2008; Wilson et al, 2008). Two P150cm plates of cells were used for each ChIP. Cells were cultured in RPMI media supplemented with 10% charcoal dextran stripped FBS for 72 before adding 1nM R1881 or 0.01% ethanol for four hours. DNA protein interactions were cross-linked using 1% formaldehyde for 10min at room temperature, before quenching with a final concentration of 125mM glycine. Cells were harvested by scraping and washed twice with 10ml 1x PBS. Nuclear lysates were isolated by incubating cells for 10min at 4oC in 10ml of LB1 (50mM Hepes-KOH, 140mM NaCl, 1mM EDTA, 10% glycerol, 0.5% Igepal, 0.25% Triton X-100), pelleting nuclei at 1300g for 5min at 4oC, washing nuclei in 10ml LB2 (10mM Tris-HCl pH8, 200mM NaCl, 1mM EDTA, 0.5mM EGTA) at 4oC for 5min, pelleting nuclei as before and adding 1ml LB3 (10mM Tris-HCl pH8, 100mM NaCl, 1mM EDTA, 0.5mM EGTA, 0.1% Sodium Deoxycholate, 0.5% N-lauroylsarcosine). Nuclear lysates were divided into four 250ul fractions, sonicated for 15min (30sec on, 30sec rest) at maximum power in a Bioruptor sonication waterbath (Diagenode), recombined (total volume 1ml), 100ul of 10%Triton X-100 was added and insoluble debris was removed by centrifugation at 20,000g for 10min at 4oC. Supernatants were diluted with 2ml of LB3 and 200ul 10% Triton X-100, 50ul was taken as total input control and the remainder was used for ChIP.

For each ChIP reaction 75ul protein-A and 75ul protein-G magnetic beads (Dynal, Invitrogen) were washed three times with 0.5% BSA in 1x PBS, before incubation overnight with 10ug of specific antibody (AR N20 [SC-816X, Santa Cruz] or phosphor-Ser-5 RNAP II [AB-5401, Abcam]) overnight at 4^{o}C with gentle agitation. Antibody-bead complexes were washed three times in 1ml 0.5% BSA 1x PBS, resuspended in 100ul of the same buffer, combined with the pre-cleared nuclear lysates and incubated overnight at 4^{o}C with gentle agitation. The following day bead-antibody-protein-DNA complexes were washed five times in RIPA buffer (50mM Hepes-KOH pH 7.6, 500mM LiCl, 1mM EDTA, 1% Igepal, 0.7% Sodium Deoxycholate), once with TE plus 50mM NaCl at 4^{o}C and eluted in 200ul elution buffer (50mM Tris-HCL pH8, 10mM EDTA, 1% SDS) for 15min at 65^{o}C with vortexing. Cross-links were reversed overnight at 65^{o}C. RNA and proteins were degraded by adding 200ul of TE and 8ug of DNAse-free RNAse A (Ambion), incubation for 30min at 37^{o}C, followed by addition of 80ug Proteinase K (Invitrogen) and incubation at 55^{o}C for 1h. Genomic DNA was isolated using phenol:chloroform:isopropanol (25:24:1, Invitrogen), back-extracted with 200ul of TE, precipitated with isopropanol, washed with 75% ethanol, air-dried and resuspended in 60ul 10mM Tris-HCl pH 8. ChIP enrichment was tested by Realtime PCR using 6ul of DNA and the remainder was used for single-end SOLEXA library preparation.

ChIP-seq SOLEXA library preparation

Single-end SOLEXA sequencing libraries were prepared as previously described (Schmidt et al, 2008). Briefly, 54ul of ChIP DNA or 50ng of total input control DNA were subjected to end-repair using T4 DNA polymerase, Klenow DNA polymerase and T4 polynucleotide kinase, before purification using the DNA Clean and concentrator-5 kit (Zymo Research).

Adenine overhangs were added using Klenow 5'-3' exo-minus, Illumina Solexa sequencing adapters were ligated using T4 DNA ligase and amplified with 18 PCR cycles using Phusion DNA polymerase (Finnzymes) and Illumina Solexa sequencing primers 1.1 and 2.1. Libraries were size selected by electrophoresis, excising the SYBR-safe, DNA smear between 200-300bp on a Dark Reader non-UV transilluminator, purified using a Qiagen gel-extraction mini-elute kit, quantified using an Agilent Bioanalyser, 36bp sequence reads were generated using a Illumina (Solexa) Genome Analyzer II and these reads were mapped back to the reference human genome before peak calling.

Sequence read analysis

Sequence reads were generated by the Illumina analysis pipeline version 1.3.4 and 1.4.0. The two lanes of reads were combined for each sample, and aligned to the Human Reference Genome (assembly hg18, NCBI Build 36.1, March 2008) using MAQ (Li et al, 2008). Next they were filtered by alignment quality score, removing all reads with a MAQ score less than 20, and exact duplicate reads were removed such that no single read start position was represented more than once. Enriched regions of the genome were identified by comparing the ChIPed samples to Input samples using two independent peak calling algorithms: MACS (Zhang et al 2008) and ChIPSeqMini (Johnson et al, 2007), taking only those regions found by both algorithms. Sites found in the androgen-stimulated condition, but not the vehicle treated condition, were taken forward for further analysis. All ChIP-seq data have been deposited at the NCBI Short Read Archive (SRA012454.1) and identified binding sites (peaks) are available in **Supplementary Tables 1-3**. The 'super-set' of AR binding sites (**Supplementary Tables 3**) was generated by combining the publicly available AR peak regions as previously reported in supplementary files, the main text of articles and from online repositories associated with the previous AR ChIP studies (Barski et al, 2007; Bolton

et al, 2007; Horie-Inoue et al, 2004; Horie-Inoue et al, 2006; Jariwala et al, 2007; Jia et al, 2008; Lin et al, 2009; Massie et al, 2007; Takayama et al, 2007; Wang et al, 2009).

Overlap, subtraction, union and feature annotation of ChIP-seq enriched regions were done using the Galaxy website (Blankenberg et al, 2007; Taylor et al, 2007). Transcription factor motifs were identified using CEAS, *de novo* motif searches (MEME and Nested MICA) (Bailey & Elkan, 1995; Down & Hubbard, 2005) and position weight matrix searches (RSAT, matrix-scan. http://rsat.ulb.ac.be/rsat/). Motifs identified using *de novo* searches were aligned with known transcription factor PWMs using the motif alignment tool in the JASPAR database (http://jaspar.cgb.ki.se/).

Illumina beadarrays

48 total RNA samples were harvested from LNCaP cells grown for 72h in steroid depleted medium (RPMI supplemented with 10% charcoal dextran stripped FBS). These comprised: 3 time zero samples; 10 vehicle (ethanol) control samples taken at 2h, 4h, 8h, 12h, 24h in duplicate; 36 androgen (R1881) treated samples taken every 30min for 4h then every hour until 24h following treatment (with replicates at 1h, 2h, 4h, 8h, 12h, 16h, 20h, 24h). Total RNA was extracted using Trizol and isopropanol precipitation, according to the manufacturers instructions. Quality control was performed with an Agilent Bioanalyser. cRNA was generated and biotin labelled using the Illumina TotalPrep RNA Amplification Kit, according to the manufacturers instructions. Hybridization and scanning were performed using Standard Illumina protocols.

Autocorrelation analysis of Illumina gene expression data

The Illumina HumanWG v2 BeadArrays consist of two replicate sections that we treat as technical replicate arrays for the purposes of this analysis due to small but systematic shifts between sections that need to be addressed in the normalization. Data were analysed from the raw bead-level using the beadarray software, with spatial artefacts identified and removed automatically (BASH) and curated manually (Cairns et al, 2008; Dunning et al, 2007). The resultant, reduced, data set was then summarized in a standard fashion (with outliers removed) in order to obtain a mean log-intensity and standard error for each probe/array combination. The November 2008 annotation from http://www.compbio.group.cam.ac.uk/Resources/Annotation/index.html was used to map probes to transcripts, and probes with no "good" or "perfect" match were discarded along with those that registered no signal above background on all 96 arrays. This resulted in 17182 probes for which analysis proceeded.

To detect probes that showed a systematic, smooth, change over time without prescribing a form for that change we used the autocorrelation at lag 1 as a measure of activity. This measure identifies profiles where neighbouring time-points are more similar than disparate time points, and so can identify all smooth and systematic gene expression changes regardless of the shapes of their profiles. To account for the uncertainty in our measurements, we simulated 100 sets of observations from the known means and standard errors, calculated the autocorrelation of each and took the mean. Simulations, and arguments of symmetry suggested that a cut-off of autocorrelation=0.5 would lead to a low false-discovery rate and 4224 probes passed this threshold. Standard clustering methods were then used to group these 4224 probes into 20 clusters of similar expression profiles. Since 98% of probes were grouped within the first six clusters these were subdivided into further sub-clusters of similar

expression profiles. Of the 4224 probes with an acf score >0.5 there were 905 which were grouped into clusters showing little change in response to androgens (sub-clusters: 1-2, 1-6, 1-9, 2-3, 4-2, 4-5, 4-8, 4-9, 6-2, 6-4, 6-5, 6-7, 6-13) and as a further filter on the gene expression data these were excluded from further analysis, leaving 3319 probes with changes in response to androgens. Raw and normalised data from Illumina BeadArray experiments have been deposited at GEO (under accession GSE18684).

Functional annotation was done using the DAVID gene ontology tool and interaction networks were generated using Cytoscape with the BiNGO and BioNetBuilder plug-ins.

Realtime PCR validation

We used quantitative Realtime PCR to confirm AR binding sites and gene expression changes using the primers listed below (**SM Table 2**), using SYBRgreen chemistry (Applied Biosystems, 2x SYBRgreen master mix) in an ABI7900 instrument (Applied Biosystems).

Primer Name	Sequence	Application
FRAP1 qrt-1F	TTACAGGCCTGGATGGCAACTACA	gene expression
FRAP1 qrt-1R	TTGTGTCCATCAGCCTCCAGTTCA	gene expression
FRAP1 qrt-2F	TCCTTGGCACAACAGTGCATTGAC	gene expression
FRAP1 qrt-2R	GGACAGCATGTGGCAAGAAACCAT	gene expression
FRAP1 ChIP -142kb-F	ACATGCTCAGAACAGAGCTGCCTA	AR ChIP
FRAP1 ChIP -142kb-R	AGCAGGAATCTAAACCCTGGCAGT	AR ChIP
FRAP1 ChIP +9kb-F	TCTGAGGACAGAGGAAGGAAAGCA	AR ChIP
FRAP1 ChIP +9kb-R	CCAGGTAGAGTTCTAGGCTGTTAG	AR ChIP
FRAP1 ChIP +104kb-F	AATCCTGGAGCTAATGGCCACCTT	AR ChIP
FRAP1 ChIP +104kb-R	ATTGAGACAAGGACTCCGCAGACA	AR ChIP

FRAP1 +129kb-F	CATGAGCTTGTGCAGTTCCTGCTT	AR ChIP
FRAP1 +129kb-R	TACAGATCGATGCCTTCCAGCACA	AR ChIP
PSA/KLK3 promoter F1	GTTGGGAGTGCAAGGAAAAG	AR ChIP
PSA/KLK3 promoter R1	CCAGCACTCAGGAGATTGTG	AR ChIP
PSA/KLK3 promoter F2	TCTGCCTTTGTCCCCTAGAT	AR ChIP
PSA/KLK3 promoter R2	AACCTTCATTCCCCAGGACT	AR ChIP
PSA/KLK3 -4kb enhancer-F2	AGGACAGTCTCAACGTTCCACCAT	AR ChIP
PSA/KLK3 -4kb enhancer-F2	TGCCTTATTCTGGGTTTGGCAGTG	AR ChIP
PSA/KLK3 -4kb enhancer-F1	TGCCACTGGTGAGAAACCTGAGAT	AR ChIP
PSA/KLK3 -4kb enhancer-F1	TCAGAGACAAAGGCTGAGCAGGTT	AR ChIP
PSA/KLK3 -12.5kb enhancer-F	AGGTGGATCAGCAGTCCGACATAA	AR ChIP
PSA/KLK3 -12.5kb enhancer-R	CACACAGTGGTTTGCGTCAATGCT	AR ChIP
EGFR-F		
EGFR-R	GGTCACAGGAACATTGCAGCTGAT	AR ChIP
SLC45A3-F	AGCTTTGGGTGGCCCATTATAACC	AR ChIP
SLC45A3-R	TTGCTTTCTTCCCTACTCCCACCT	AR ChIP
ZBTB16-F	ACATGCTTGTCTATCCAGTGCCAG	AR ChIP
ZBTB16-R	ATGCCCTGCGTCTGTACTCATTGT	AR ChIP
GRHL2-1-F	TGTTCTGATGAGATCTGCACGCCT	AR ChIP
GRHL2-1-R	AGCCTCTCAAGCAGGTTTCTGACA	AR ChIP
GRHL2-2-F	AATAACCTGTCCGGCCCAAGAGAA	AR ChIP
GRHL2-2-R	ACTACTTTCTGGTGCAGATGTTCC	AR ChIP
ACSL3-F	ATCACAACCTGTACTGCCCGTTCT	AR ChIP
ACSL3-R	AGTCCCAGGAACAGAAAGGCATGA	AR ChIP
	TCCTTTGATCGCTGGGTGTTGACT	AR ChIP
CAMKK2 qrt-F	TGAAGACCAGGCCCGTTTCTACTT	gene expression
CAMKK2 qrt-R	TGGAAGGTTTGATGTCACGGTGGA	gene expression
CAMKK2 -2kb promoter F1	AGAACACTGTAGCTCACACAGGCA	AR ChIP
CAMKK2 -2kb promoter R1	GGGCACTTCCCAACCTTTCTTACT	AR ChIP

CAMKK2 -2kb promoter F2	AAGATTGGGCCATTGCACTCTAGC	AR ChIP
CAMKK2 -2kb promoter R2	TGATCATATCCTGGTCTTCTGCCC	AR ChIP

Table 1 Primers used for Realtime PCR validation.

Immunohistochemistry

Paraffin embedded sections were deparaffinised and rehydrated. Antigen retrieval was performed by microwaving the slides in Tris/EDTA buffer (pH9.0) for 15mins. The slides were incubated with normal donkey serum for 1hr before incubation with the primary antibody (CAMKK2: Atlas Antibodies #HPA017389) at a 1:100 dilution for 1hr at room temperature. The slides were then incubated with a biotinylated IgG secondary antibody (Jackson Immuno Research) for 1hr followed by a streptavidin-biotin-peroxidase detection system (Vectastain Elite ABC Kit). The slides were then visualised using 3,3'-diaminobenzadine (Vector laboratories, SK-4100) and counterstained with haematoxylin.

Xenograft experiments

Xenograft tumours were generated with C4-2b cells that stably expressed a fusion protein of luciferase and YFP. Ice cold high concentration matrigel (BD Biosciences) was mixed with an equal volume of a cell suspension of 4xE7 cells in ice cold PBS prior to injecting. NOD SCID Gamma (NSG) male mice were injected in the caudal flank regions with 0.1 ml of the cell suspension/Matrigel mixture (2xE6 cells) using a 25 gauge needle. The castrations were performed the same day using isoflurane for the anaesthesia. There were four groups of mice (castration + vehicle, castration + STO-609, full + vehicle, full +STO-609), each consisting of four mice. 10 μmol/kg of STO-609 (or the equivalent vehicle, 10% DMSO in PBS) was

injected intraperitoneally 3 times per week and the growth of the tumours was monitored weekly though bioluminescence with an IVIS camera (Xenogen). Imaging was always performed during a day when no STO-609 or vehicle had been injected. Mice were injected intraperitoneally with 150 mg/kg of luciferin (Caliper) in PBS prior to imaging and were anaesthetised during this process with isoflurane.

Pharmacokinetic / Pharmacodynamic measurements

For plasma studies mice (**Figure S17a**) were injected IV or IP with 0.5μmol/kg STO-609 and at timepoints (5, 15, 30, 45min, 1, 1.5, 2, 4, 6hr) after treatment blood samples were collected into heparinised tubes. Blood was centrifuged to obtain the plasma fraction and frozen at -80^{o}C prior to analysis. For tumour and parallel serum measurements (**Figure S17b**) mice were treated with 10 μmol/kg and samples of blood and tumour were collected at 0.5 and 2hr after treatment. Bioanalysis was carried out by protein precipitation of plasma followed by detection using a STO-609 specific LC-MS/MS method with an assay range of 1 to 1000 ng/mL. The plasma concentration:time profile was then constructed for PK analysis by WinNonLin. Tumour samples were homogenised 4 v/w in 50% CH_3CN (aq). An aliquot of this homogenate then processed using the same extraction procedure as plasma. The assay range for STO609 in tumour homogenate was 4 to 4000 ng/g.

Metabolomic profiling

LNCaP cells grown in RPMI media supplemented with 10% FBS were harvested on day zero, days1, 2 and 3 after DMSO or STO-609 treatment. LNCaP cells grown in RPMI media supplemented with 10% charcoal dextran treated (steroid depleted) FBS were harvested on

day zero, days1, 2 and 3 with and without androgen treatment (1nM R1881). Cell media was collected from all the cell plates for NMR analysis. Metabolites from the cells were extracted by following protocol. After taking the media cells were washed twice with sterile 3ml physiological saline. 2ml ice cold 6% PCA was added and cells were scrapped into a centrifuge. Scrapped cells were centrifuged at 1000RPM for 10 min at 4° C. Supernatant was taken and neutralised to pH 7 with KOH and PCA. Cell number and cell protein content were estimated. After neutralisation and lyophilisation these samples were re-suspended in 1 ml of D_2O for ^1H NMR analysis. 600 µl of the sample was taken in a 5 mm standard wilmad NMR tube 10 µL of 10 mM TSP was added as external standard. ^1H NMR spectroscopy data was acquired on a 600 MHz Bruker Avance NMR spectrometer. We have used a water pre-saturation sequence with 128 averages, repetition time=5sec and 64K time domain data points. Pre-processing of the time domain data included exponential multiplication (line broadening 0.3 Hz), Fourier transformation, zero and first order phase correction. TSP was used for chemical shift calibration and metabolite quantitation. Metabolite concentrations were normalized to the protein content of cells.

^1H NMR spectra were binned, in AMIX software, with 0.05 ppm intervals and the water region was omitted from the data. Unsupervised pattern recognition method Principal Component Analysis (PCA) was performed to the glog transformed data by using SIMCA software package.

Glucose flux experiments using 1,2-13C2-Glucose and GC/MS

Cells were grown in media supplemented with charcoal dextran treaded FBS (steroid depleted conditions) and treated either with vehicle (0.01% ethanol), androgen (1nM R1881), androgen + STO-609 (25uM) or androgen + CAMKK2 siRNA for 72h. Cells were harvested

by scraping on ice and metabolites were obtained by methanol/chloroform extraction (Wu et al, 2008). The aqueous phase was dried using a Speedvac and derivatized by silylation (Perroud et al, 2006). RNA ribose extraction and derivatization was performed as previously described (Boren et al, 2003). The sample was injected into a GC-TOF MS (Leco Pegasus HT GC/TOFMS; Leco UK, Stockport, UK) and run according to methods described previously (Perroud et al, 2006). The obtained chromatograms were analyzed using the ChromaTOF software package (Leco UK) to identify the different peaks. Mass spectral results were accepted only if the standard sample deviation was less than 1% of the normalized peak intensity.

Phosphofructokinase activity measurements

PFK activity was measured in prostate cancer cell line extracts using the method of Brand and Solings, 1974 (Brand & Soling, 1974). Briefly, cells were grown for three days in media supplemented with the CAMKK2 inhibitor STO-609 (10uM), the anti-androgen casodex (10uM) or vehicle controls (DMSO and ethanol). Cells were washed twice with ice cold PBS and harvested on ice using a cell scraper in PFK reaction buffer (50mM HEPES pH7.4, 100mM KCl, 10mM NaH_2PO_4, 10mM $MgCl_2$). Cells suspensions were sonicated for 10min (30sec on, 30sec rest) at maximum power in a Bioruptor sonication waterbath (Diagenode) and centrifuged at 31,000g for 30min at 4^{o}C. The reaction mixture (containing 2mM NADH, 3mM Fructose-6-phosphate, 2mM ATP, 3.5 U/ml Triosephosphate Isomerase, 0.5 U/ml α-Glycerophosphate Dehydrogenase, 0.3 U/ml aldolase) was pre-incubated at 37^{o}C for 2 min. PFK activity reactions were started by adding cell extracts (1mg/ml), incubation at 37 ^{o}C and NADH levels were measured continuously for 5 min using OD 340nm. The slope of NADH

loss (OD 340nm) was used to calculate PFK levels in cell lysates from different treatment conditions, in international units per milligram of protein in cell lysates (UI/mg).

Glucose and Lactate measurements

Media was harvested from cells grown in RMPMI supplemented with either 10% FBS or 10% charcoal dextran treated FBS and treated for 3 days with or without androgen, bicalutamide (casodex) or ST0-609. Glucose and lactate levels were determined using commercial enzyme based kits (BioVision Inc., US).

Oxygen consumption

Cells were grown in completed media or media supplemented with 10% charcoal dextran treated FBS, treated with vehicle (0.01% ethanol), androgen (1nM R1881), bicalutamide (10μM), STO609 (25μM), metformin (5mM) or oligomycin (1mM). Cells were harvested using trypsin, counted using a ViCell cytometer and resuspended in at 10^6 cells / ml. Oxygen consumption of cell suspensions were measured using a Clark-type oxygen electrode (DW1 Oxygen Electrode Chamber, Hansatech) over a 15min time course at 37^{o}C, according to the manufactures instructions. The oxygen electrode was calibrated using air saturated water and a saturated solution of Sodium Sulfite. Oligomycin was used as a positive control for respiratory chain inhibition. Triplicate measurements were made for each treatment condition and O_2 consumption rates were calculated using the OxygraphPlus software (Hansatech), expressed as nmol/ml/min.

References

Bailey TL, Elkan C (1995) The value of prior knowledge in discovering motifs with MEME. *Proc Int Conf Intell Syst Mol Biol* **3:** 21-29

Barski A, Cuddapah S, Cui K, Roh TY, Schones DE, Wang Z, Wei G, Chepelev I, Zhao K (2007) High-resolution profiling of histone methylations in the human genome. *Cell* **129**(4)**:** 823-837

Blankenberg D, Taylor J, Schenck I, He J, Zhang Y, Ghent M, Veeraraghavan N, Albert I, Miller W, Makova KD, Hardison RC, Nekrutenko A (2007) A framework for collaborative analysis of ENCODE data: making large-scale analyses biologist-friendly. *Genome research* **17**(6)**:** 960-964

Bolton EC, So AY, Chaivorapol C, Haqq CM, Li H, Yamamoto KR (2007) Cell- and gene-specific regulation of primary target genes by the androgen receptor. *Genes Dev* **21**(16)**:** 2005-2017

Boren J, Lee W-NP, Bassilian S, Centelles JJ, Lim S, Ahmed S, Boros LG, Cascante M (2003) The Stable Isotope-based Dynamic Metabolic Profile of Butyrate-induced HT29 Cell Differentiation. *J Biol Chem* **278**(31)**:** 28395-28402

Brand IA, Soling HD (1974) Rat liver phosphofructokinase. Purification and characterization of its reaction mechanism. *J Biol Chem* **249**(24)**:** 7824-7831

Cairns JM, Dunning MJ, Ritchie ME, Russell R, Lynch AG (2008) BASH: a tool for managing BeadArray spatial artefacts. *Bioinformatics* **24**(24)**:** 2921-2922

Down TA, Hubbard TJ (2005) NestedMICA: sensitive inference of over-represented motifs in nucleic acid sequence. *Nucleic Acids Res* **33**(5)**:** 1445-1453

Dunning MJ, Smith ML, Ritchie ME, Tavare S (2007) beadarray: R classes and methods for Illumina bead-based data. *Bioinformatics* **23**(16)**:** 2183-2184

Horie-Inoue K, Bono H, Okazaki Y, Inoue S (2004) Identification and functional analysis of consensus androgen response elements in human prostate cancer cells. *Biochemical and biophysical research communications* **325**(4)**:** 1312-1317

Horie-Inoue K, Takayama K, Bono HU, Ouchi Y, Okazaki Y, Inoue S (2006) Identification of novel steroid target genes through the combination of bioinformatics and functional analysis of hormone response elements. *Biochemical and biophysical research communications* **339**(1)**:** 99-106

Jariwala U, Prescott J, Jia L, Barski A, Pregizer S, Cogan JP, Arasheben A, Tilley WD, Scher HI, Gerald WL, Buchanan G, Coetzee GA, Frenkel B (2007) Identification of novel androgen receptor target genes in prostate cancer. *Mol Cancer* **6:** 39

Jia L, Berman BP, Jariwala U, Yan X, Cogan JP, Walters A, Chen T, Buchanan G, Frenkel B, Coetzee GA (2008) Genomic androgen receptor-occupied regions with different functions, defined by histone acetylation, coregulators and transcriptional capacity. *PLoS One* **3**(11)**:** e3645

Johnson DS, Mortazavi A, Myers RM, Wold B (2007) Genome-wide mapping of in vivo protein-DNA interactions. *Science* **316**(5830)**:** 1497-1502

Li H, Ruan J, Durbin R (2008) Mapping short DNA sequencing reads and calling variants using mapping quality scores. *Genome research* **18**(11)**:** 1851-1858

Lin B, Wang J, Hong X, Yan X, Hwang D, Cho JH, Yi D, Utleg AG, Fang X, Schones DE, Zhao K, Omenn GS, Hood L (2009) Integrated expression profiling and ChIP-seq analyses of the growth inhibition response program of the androgen receptor. *PLoS One* **4**(8)**:** e6589

Massie CE, Adryan B, Barbosa-Morais NL, Lynch AG, Tran MG, Neal DE, Mills IG (2007) New androgen receptor genomic targets show an interaction with the ETS1 transcription factor. *EMBO reports* **8**(9)**:** 871-878

Perroud B, Lee J, Valkova N, Dhirapong A, Lin PY, Fiehn O, Kultz D, Weiss RH (2006) Pathway analysis of kidney cancer using proteomics and metabolic profiling. *Mol Cancer* **5:** 64

Schmidt D, Stark R, Wilson MD, Brown GD, Odom DT (2008) Genome-scale validation of deep-sequencing libraries. *PLoS One* **3**(11)**:** e3713

Takayama K, Kaneshiro K, Tsutsumi S, Horie-Inoue K, Ikeda K, Urano T, Ijichi N, Ouchi Y, Shirahige K, Aburatani H, Inoue S (2007) Identification of novel androgen response genes in prostate cancer cells by coupling chromatin immunoprecipitation and genomic microarray analysis. *Oncogene* **26**(30)**:** 4453-4463

Taylor J, Schenck I, Blankenberg D, Nekrutenko A (2007) Using galaxy to perform large-scale interactive data analyses. *Curr Protoc Bioinformatics* **Chapter 10:** Unit 10 15

Wang Q, Li W, Zhang Y, Yuan X, Xu K, Yu J, Chen Z, Beroukhim R, Wang H, Lupien M, Wu T, Regan MM, Meyer CA, Carroll JS, Manrai AK, Janne OA, Balk SP, Mehra R, Han B, Chinnaiyan AM, Rubin MA, True L, Fiorentino M, Fiore C, Loda M, Kantoff PW, Liu XS, Brown M (2009) Androgen receptor regulates a distinct transcription program in androgen-independent prostate cancer. *Cell* **138**(2)**:** 245-256

Wilson MD, Barbosa-Morais NL, Schmidt D, Conboy CM, Vanes L, Tybulewicz VL, Fisher EM, Tavare S, Odom DT (2008) Species-specific transcription in mice carrying human chromosome 21. *Science* **322**(5900)**:** 434-438

Wu H, Southam AD, Hines A, Viant MR (2008) High-throughput tissue extraction protocol for NMR- and MS-based metabolomics. *Analytical Biochemistry* **372**(2)**:** 204-212

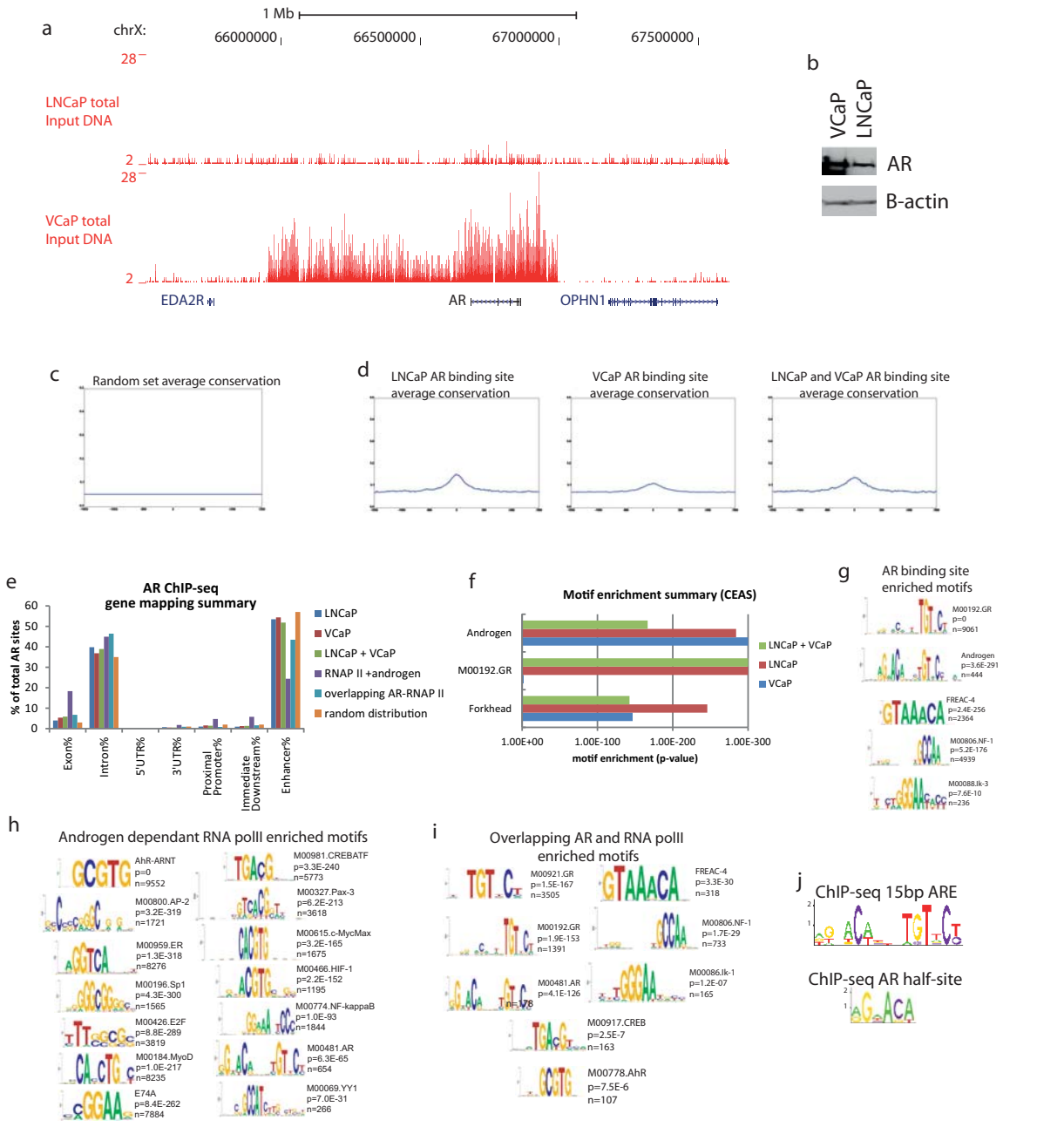

Supplementary Figure 1 Analysis of androgen dependent AR and RNAP II enriched sites. (a) Total genomic DNA sequencing from LNCaP and VCaP cell lines, showing the genomic amplification of the AR locus in VCaP cells. (b) Western blot for the AR (N20) and beta-actin using LNCaP and VCaP cell lysates. (c) Conservation plot of background genome using a random set from the Broad Align mappable 36bp sequences track (downloaded from the UCSC Genome browser). (d) Conservation plots of all androgen dependant AR binding sites. (e) Gene mapping location analysis of AR ChIP-seq enriched sites, androgen dependant RNAP II enriched sites, overlapping AR and androgen dependant RNAP II sites and a random set of regions (from Broad mappable 36bp set). (f) Enrichment analysis of androgen receptor motifs, GR 6bp motifs and forkhead bininding motifs in AR binding sites identified in LNCaP, VCaP and the common targtes identified in both cell lines. (g) Motifs enriched in androgen dependant AR binding sites (p denotes p-value, n denotes number of motifs found). (h) Motifs enriched in androgen dependant RNAP II sites. (i) Motifs enriched in overlapping AR and RNAP II sites (no enriched sequence motifs were identified using the random set of coordinates). (j) Sequence motifs from de novo motif analysis of AR binding sites (MEME). Data for conservation, location analysis and motif enrichment were generated using CEAS (Cis-regulatory Element Annotation System).

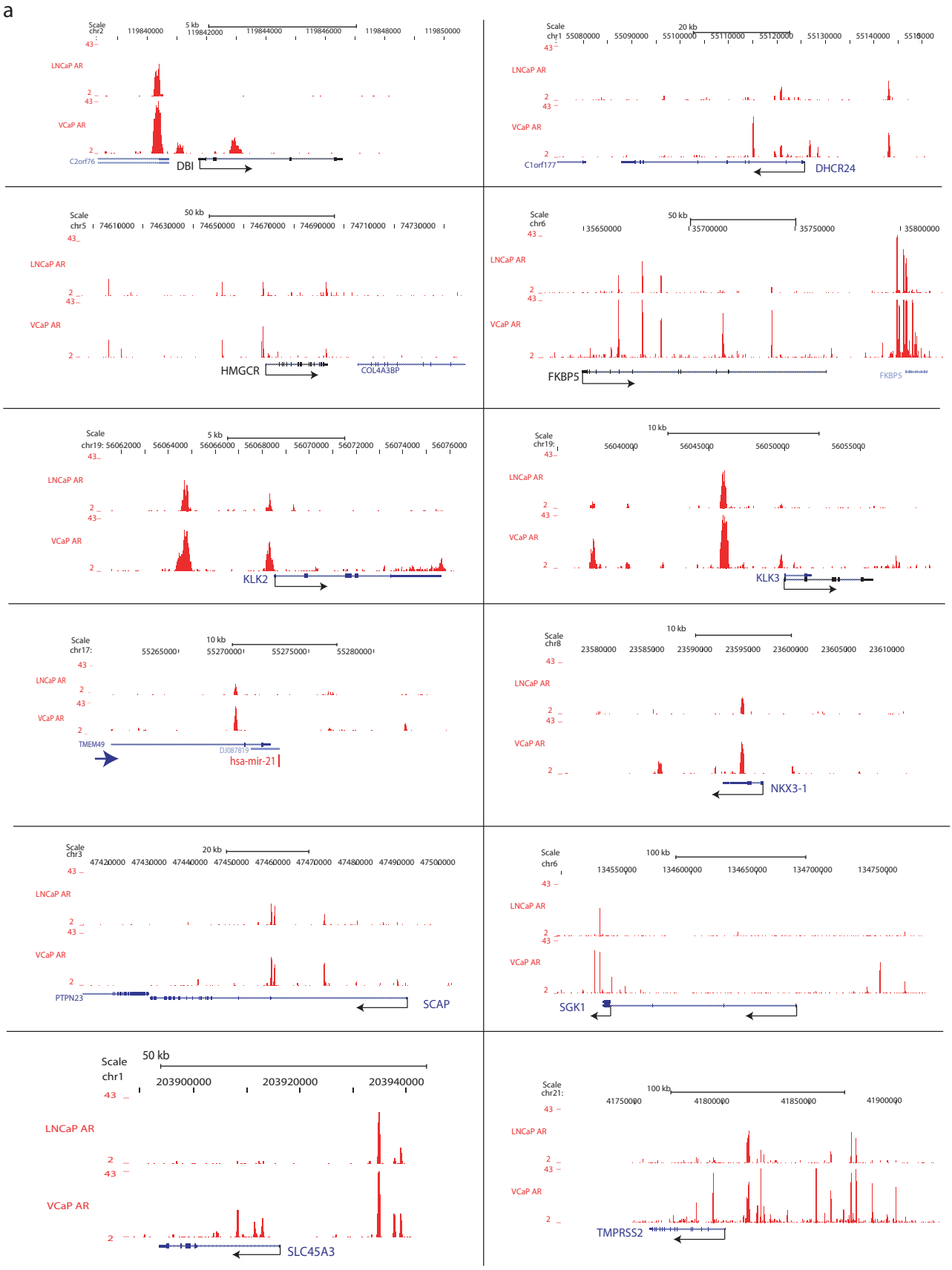

Supplementary Figure 2 Summary of known AR binding sites and validation of a panel of novel AR target sites identified using ChIP-seq. (a) AR ChIP-seq enrichment in both LNCaP and VCaP cells of known AR target genes, as annotated. AR enrichment is shown in red, genes are indicated below and arrows indicate the direction of transcription. (b) Heatmap showing AR ChIP enrichment assessed with qPCR for a panel of AR binding sites identified using AR ChIP-seq (average of triplicates, AR ChIP in androgen stimulated cells [1nM R1881, 4h] relative to AR ChIP normalised to AR ChIP in vehicle treated cells, normalised against unbound control region).

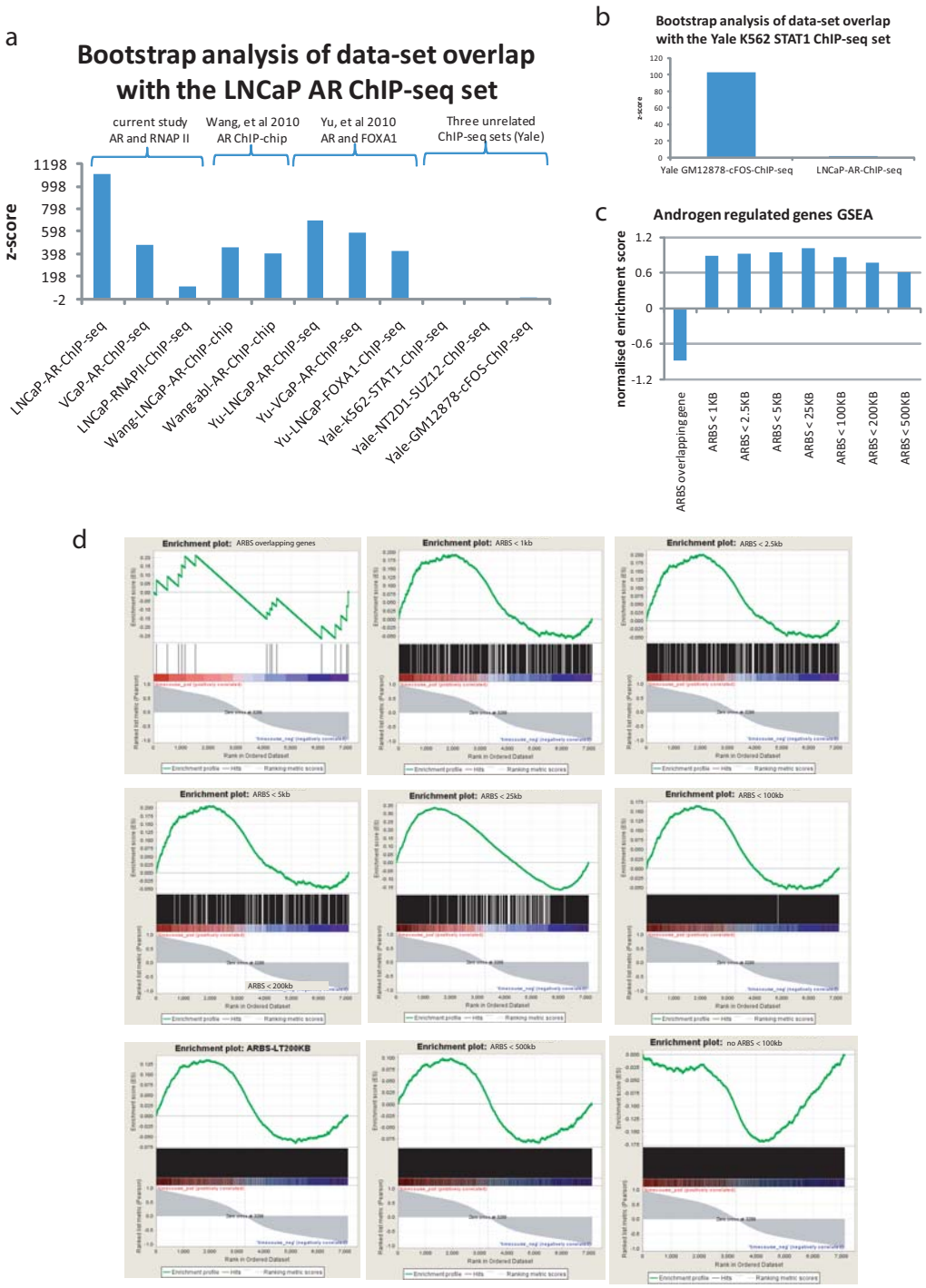

Supplemetary Figure 3 Enrichment analysis of our AR ChIP-seq data with previously published ChIP datasets and summary of GSEA (gene set enrichment analysis) to determine the optimal genomic window around AR binding sites. (a) Pair-wise comparison of LNCaP AR ChIP-seq data with other ChIP data sets indicated on the x-axis, (sub-groups indicated above the graph, for previously published AR ChIP data and with control sets derived from ChIP studies of unrelated transcription factors.) (b) Control pair-wise comparison of STAT1 ChIP-seq data with cFOS and LNCaP AR data, showing significant overlap bewteen STAT1 and cFOS data sets. Z-scores were generated using the Block Bootstrap tool downloaded from http://www.encodestatistics.org/. Published AR data were retreived from GEO (GSE14092) and http://research.dfci.harvard.edu/brownlab/datasets/. Negative control data sets were retreived from UCSC Genome Browser "Yale TFBS" ChIP-seq tracks. (c) Summary of normalised enrichment scores (NES) from GSEA analysis (from detailed plots shown below) showing the enrichment of androgen regulated genes adjacent to AR binding sites. Gene sets were constructed by identifying genes overlapping with or adjacent to AR binding sites. Gene coordinates from the RefSeq database were used to find the intersect between genes and AR binding sites or AR binding sites extended by 1kb, 2.5kb, 5kb, 25kb, 100kb, 200kb and 500kb, as indicated. Androgen regulated genes identified in our 28 time-point Illumina gene expression study were ranked in GSEA using the time-course phenotype and are indicated on the x-axis (up-regulated genes indicated by red bars and down-regulated genes indicated by blue bars). (d) Individual enrichment plots from GSEA analysis summarised in panel c.

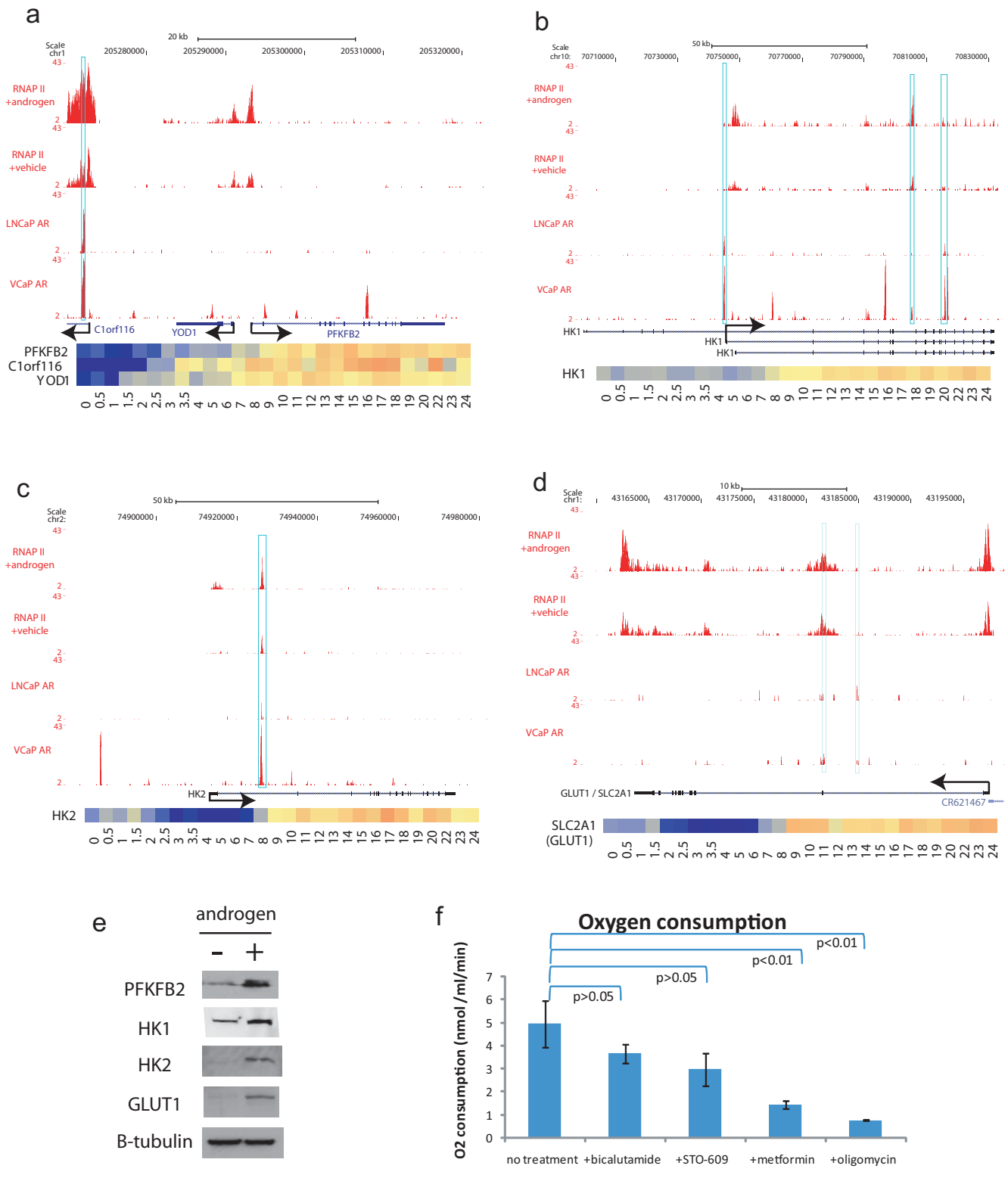

Supplementary Figure 4 AR regulation of PFKFB2, HK1, HK2 and GLUT1. (a-d) Enrichment profiles for AR and RNAP II ChIP-seq around the genes encoding (a) PFKFB2, (b) HK1, (c) HK2 and (d) GLUT1. The position of genes are indicated and arrows indicate the direction of transcription. AR and RNAP II ChIP were performed following 4h treatment with androgen (1nM R1881) or vehicle (0.01% ethanol). Androgen regulated expression is represented in the heatmaps below (data from Illumina expression array analysis). (e) Western blot analysis of LNCaP cell lysates from cells grown for 72h in steroid depleted conditions (CDT media) followed by treatment with androgen (1nM R1881) or vehicle control (0.01% ethanol). (f) Oxygen consumption rates in LNCaP cells grown for 72h in bicalutamide, STO609, metformin or oligomycin, measured using a Clark-type oxygen electrode (mean +/- S.E.M).

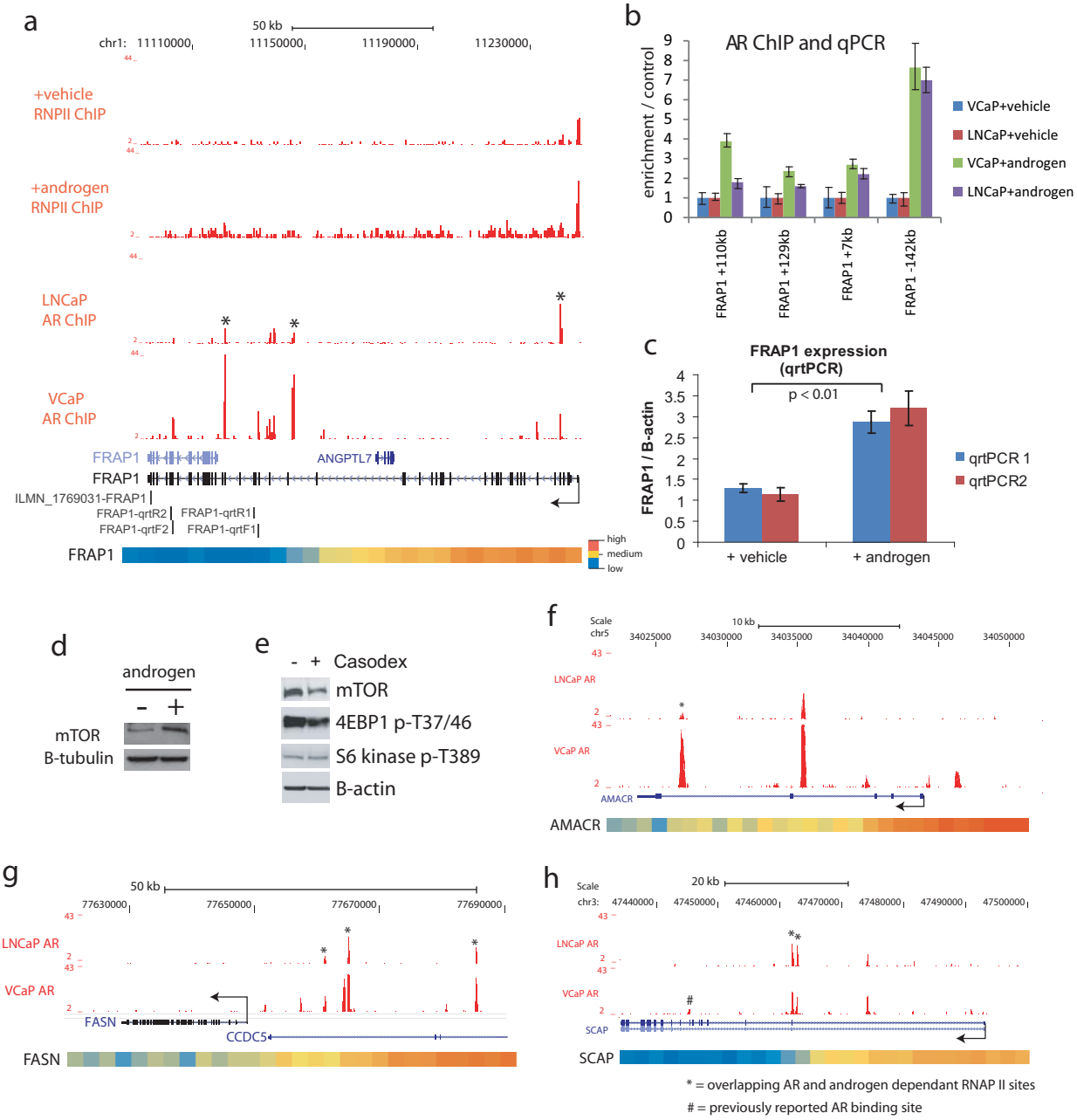

Supplementary Figure 5 AR regulation of the anabolic regulators FRAP1 (encoding mTOR), AMACR, FASN and SCAP. (a) UCSC genome browser view of the FRAP1 gene locus. RNAP II ChIP-seq enrichment is shown on the top two tracks (with and without androgens, 1nM R1881, 4h) and AR ChIP-seq peaks from LNCaP and VCaP cells are shown below (* indicates overlapping AR and RNAP II sites). Gene annotations are represented by horizontal blue and black lines, arrow indicates the direction of transcription. The genomic location of the Illumina beadarray probe and primers used for Realtime rtPCR are represented by verticle lines below. (b) AR ChIP and Realtime PCR validation of the indicated AR binding sites (distances relative to the FRAP1 transcriptional start site), following vehicle (0.01% ethanol) or androgen treatment (1nM R1881, 4h). (c) Realtime qrtPCR quantification of FRAP1 expression following control (0.01% ethanol) or androgen (1nM R1881) treatment for 24h in LNCaP cells (expressed relative to time zero for two PCR primer pairs, error-bars represent standard deviation of triplicates). (d) Western blot for mTOR and B-tubulin using lysates from LNCaP cells grown in the absence of androgens (CDT supplemented media) for 72h and then treated with androgen (1nM R1881) or vehicle control (0.01% ethanol) for 24h. (e) Western blot for mTOR and the mTOR phosphorylation targets phospho-4EBP1 and phospho-S6-kinase, with beta-actin loading control, using cell lysates from LNCaP cells treated with 10uM Casodex or vehicle control for 72h in complete medium. (f-g) UCSC genome browser view of the (f) AMACR, (g) FASN and (h) SCAP gene loci. AR ChIP-seq enrichment from LNCaP and VCaP cells are shown in red (* indicates overlapping AR and RNAP II sites). Gene annotations are represented below, arrows indicate the direction of transcription. Androgen regulated expression is shown at the bottom as a heatmap (from Illumina beadarray gene expression time-course following androgen stimulation, 1nM R1881).

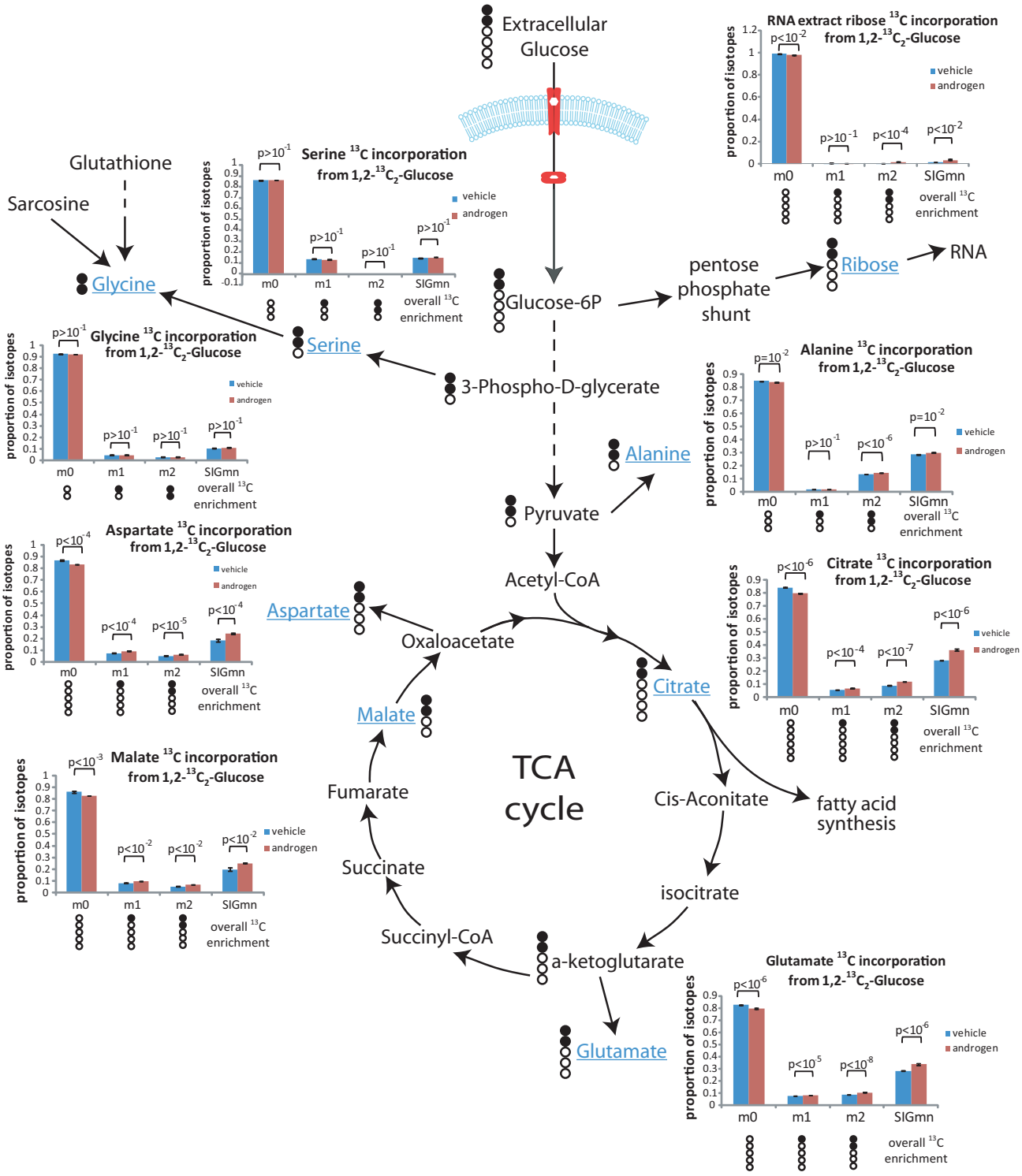

Supplementary Figure 6 Effects of androgen signalling on carbon utilization from glucose in macromolecule biosynthesis. (a) Summary of ^{13}C incorporation, as assessed by GC/MS analysis of methanol/chloroform extracted LNCaP cell lysates following 48h treatment and 24h incubation of cells with 1,2-$^{13}C_2$-glucose. Schematic shows simplified glycolysis and TCA pathways, indicating the metabolites which are converted to amino acids for protein synthesis, lipids for fatty acid synthesis and also to ribose for nucleotide synthesis. Black circles depict the carbon atoms of each measured metabolite, filled circles denote ^{13}C and open circles denote ^{12}C. The predicted ^{13}C incorporation based on glucose metabolism directly through glycolysis and the TCA cycle (NB, other routes such as the pentose phosphate pathway would result in other ^{13}C incorporation rates). Data are presented as mean of technical and biological triplicates (n=9), error bars indicate S.E.M.

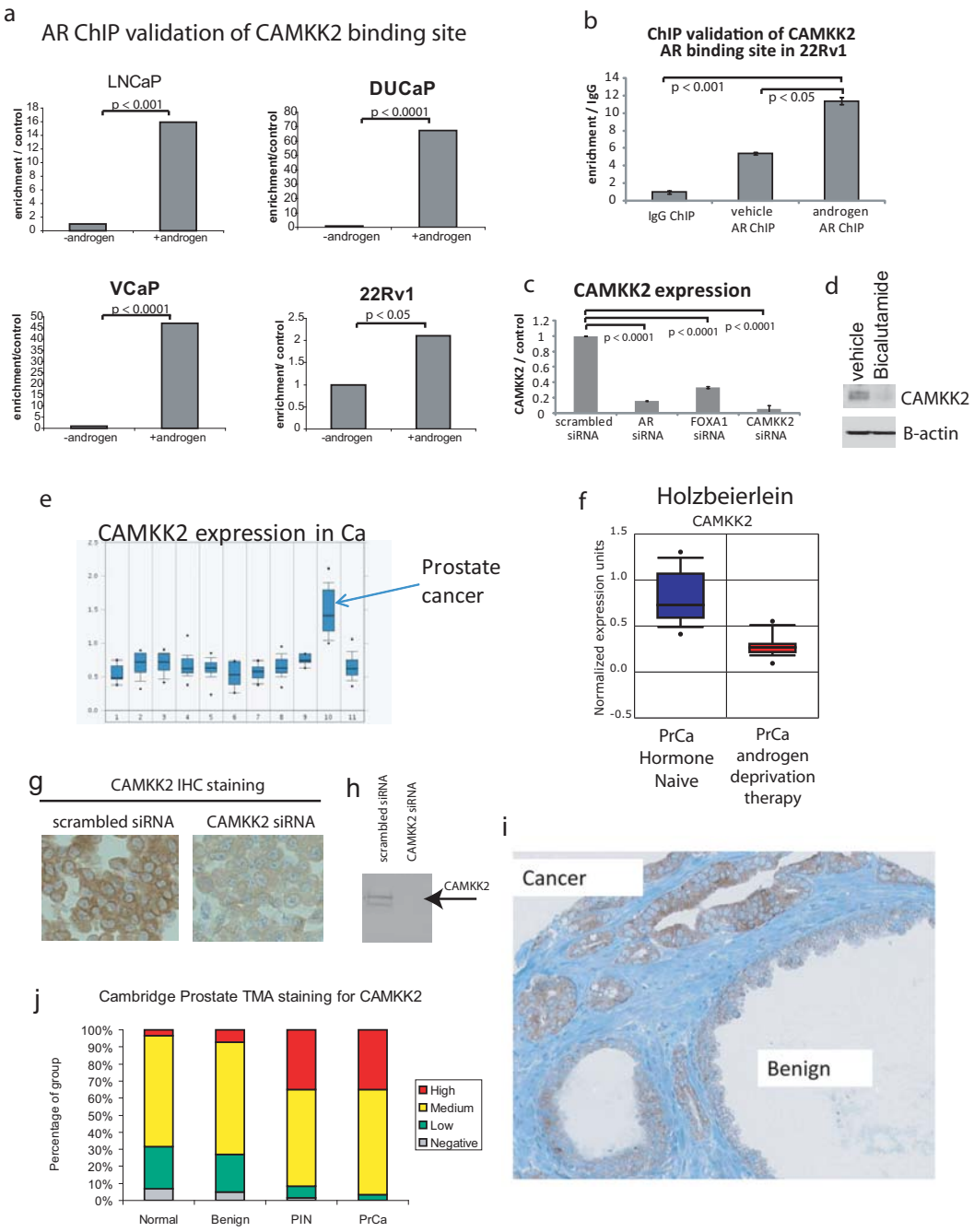

Supplementary Figure 7 Direct AR regulation of CAMKK2 and over-expression in prostate cancer. (a-b) ChIP and Realtime PCR validation of CAMKK2 AR binding site in (a) LNCaP, DUCaP, VCaP and 22Rv1 cell lines with and without androgen for 4h and (b) AR ChIP compared to IgG control ChIP for 22Rv1. (c) Realtime PCR for CAMKK2 expression 72h after transfection of scrambled siRNA, AR, FOXA1 or CAMKK2 siRNA. (d) Western blotting for CAMKK2 and B-actin using lysates from LNCaP cells treated for 72h with vehicle or the AR antagonist bicautamide (10uM). (e) Clinical gene expression data cancer vs normal sets for multiple tissue types, normal prostate vs prostate cancer highlighted (data from Oncomine). (f) Oncomine box plot showing CAMKK2 expression in hormone naive prostate cancer (PrCa) and prostate cancer post androgen ablation therapy (Holzbeierlein et al, 2004). (g) CAMKK2 IHC staining of paraffin embedded LNCaP cell pellets. Left panel shows CAMKK2 staining of scrambled control siRNA transfected cells and right panel shows staing of cells transfected with CAMKK2 siRNA. (h) Western blot for CAMKK2 using lysates from parallel transfections of LNCaP cells 72h following transfection with scrambled control or CAMKK2 siRNA. (i) Representative image of CAMKK2 IHC staining from a single section containing both benign and cancer glands. (j) Summary of CAMKK2 IHC scores for Addenbrookes 32 patient matched benign, PIN and PrCa TMA (n=318 cores).

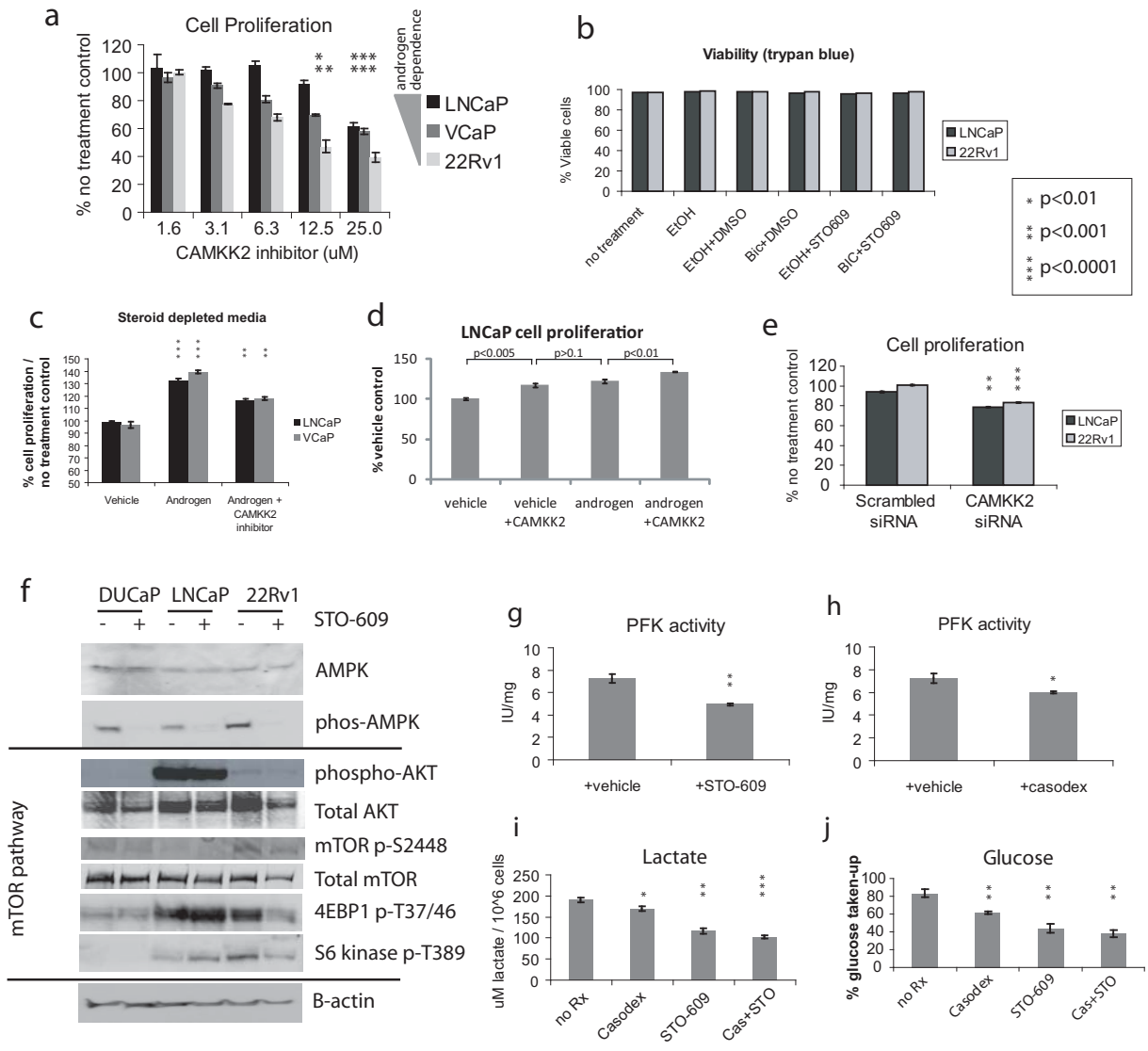

Supplementary Figure 8 Effects of CAMKK2 inhibition on proliferation, down-stream signalling and metabolism. (a) Effects of the CAMKK2 inhibitor STO-609 on prostate cancer cell line proliferation, MTS cell proliferation assay (mean of three experiments, error bars show S.E.M.). (b) Percentage viability (trypan blue exclusion) after 72h treatment of LNCaP and 22Rv1 cell lines with Casodex (10uM), CAMKK2 inhibitor (10uM STO-609) or the combined treatment. (c) Cell proliferation (MTS) assay 72h following treatment of LNCaP and VCaP cells with androgen (1nM R1881) or androgen plus the CAMKK2 inhibitor STO-609 (10μM). (d) Cell proliferation (MTS) assay showing the effects of CAMKK2 over-expression in the presence and absence of androgens (1nM R1881, 72h treatment, represented as mean +/- S.E.M). (e) Cell proliferation (MTS) assay 72h after transfection with scrambled siRNA or CAMKK2 siRNA. (error-bars show standard deviation from three biological replicates, each performed in triplicate). (f) Western blotting of lysates from DUCaP, LNCaP and 22Rv1 cell lines following 72h treatment with 10uM STO-609 or DMSO control. (g-h) Phosphofructokinase assay using LNCaP native cell lysates. Cells were grown for three days in media supplemented with STO-609 (g), casodex (h) or vehicle controls (DMSO and ethanol). PFK activity in cell lysates was measured according to the method of Brand and Sölings, 1974 (see Supplementary Methods for details). Data are represented as mean of biological triplicates and error bars show S.E.M. (i-j) Extracellular lactate (i) and glucose (j) measurents 72h following treatment of LNCaP cells with the AR antagonist casodex, the CAMKK2 inhibitor STO-609 or the combination treatment.

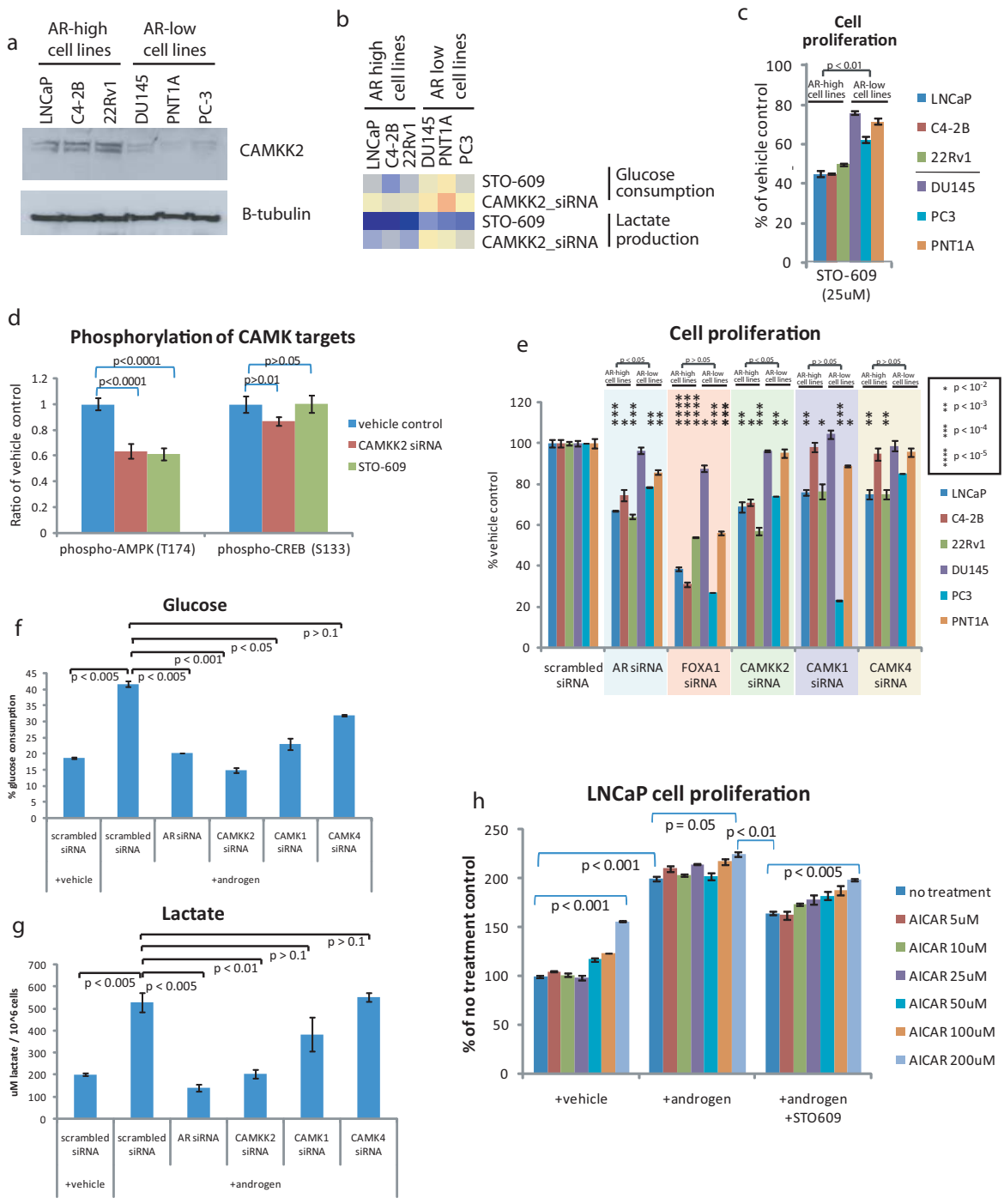

Supplementary Figure 9 The functional consequences and downstream effectors of CAMKK2 signalling in prostate cell lines which express high or low levels of the AR. (a) Western blot for CAMKK2 and beta-tubulin using lysates from AR-high cell lines (LNCaP, C4-2B, 22Rv1) and AR-low cell lines (DU145, PNT1A, PC3). (b) Heatmap showing the effects of CAMKK2 inhibition (using STO-609 or CAMKK2 siRNA) on glucose consumption and lactate production. Cells were treated for 72h and glucose and lactate were measured in cell culture media. Values are relative to vehicle control and normalised to cell number. (c) Cell proliferation following CAMKK2 inhibition using STO-609 in AR-high and AR-low expressing prosate cell lines (average of triplicates +/- SEM). (d) Quantification of the phosphorylation of CAMKK2 and CAMK1/4 targets following CAMKK2 siRNA depletion or STO-609 treatment (data from biological replicates using a phospho-proteome profiler array). (e) Cell proliferation (MTS) assay following siRNA knockdown of the AR, FOXA1, CAMKK2, CAMK1 or CAMK4 in a panel of AR-high and AR-low prostate cancer cell lines (represented as mean +/-SEM, significant changes are indicated with stars and p-values above show changes between the cell line groups). (f-g) Glucose consumption (f) and lactate production (g) in response to androgen stimulation in combination with siRNA knock-down of the AR, CAMKK2, CAMK1 or CAMK4 (data presented as mean +/- SEM of triplicate experiments, pair-wise p-values indicated above charts). (h) Cell proliferation (MTS) assay showing the effects of STO-609 treatment on androgen stimulated proliferation, with and without 5uM-200uM AICAR treatment (mean of triplicates, +/- S.E.M).

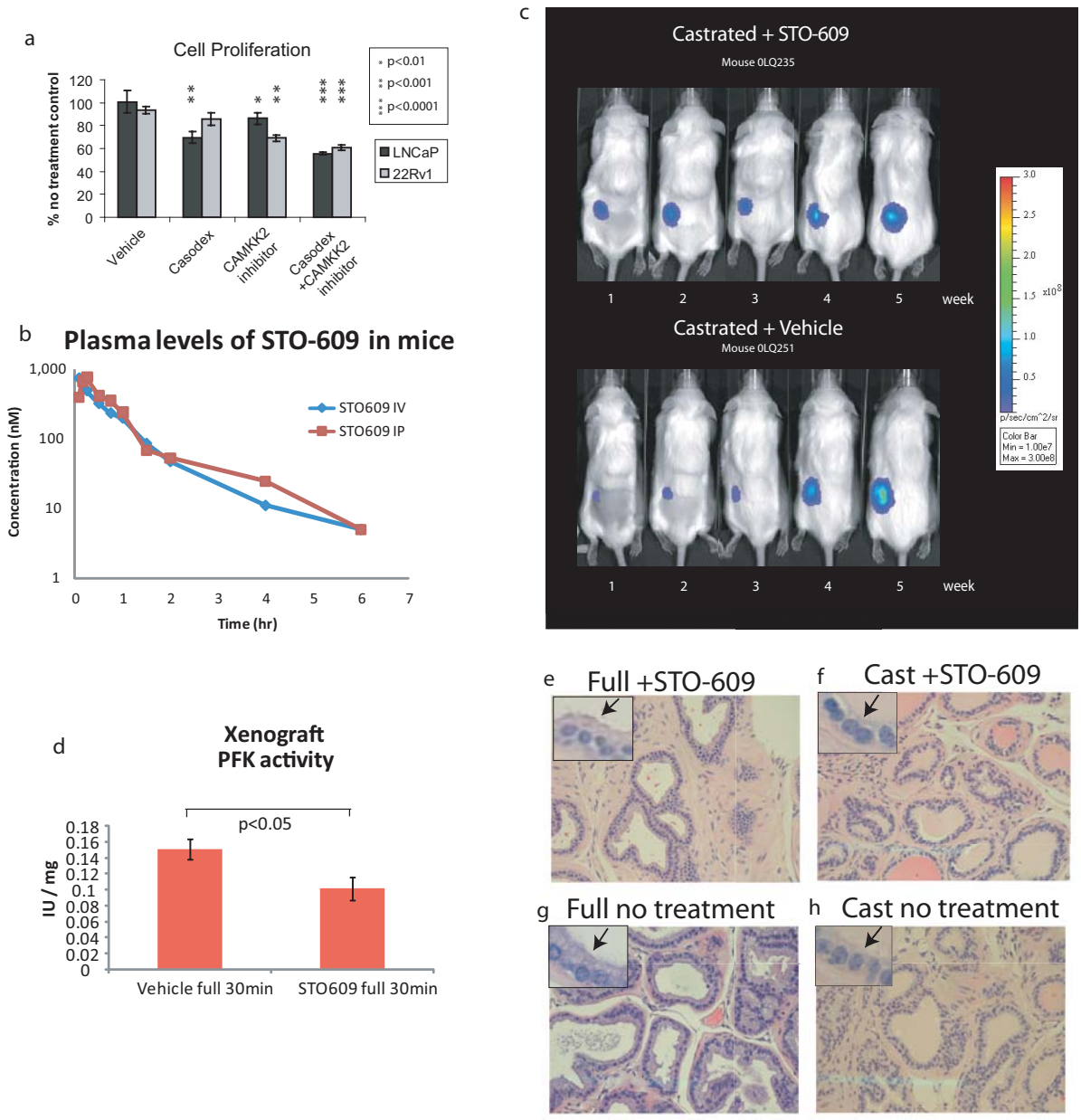

Supplementary Figure 10 In vitro and in vivo effects of CAMKK2 inhibition. (a) In vitro cell proliferation of androgen dependant LNCaP and castrate resistant 22Rv1 cell lines grown in full media (10% FBS) and treated with the anti-androgen casodex (10uM bicalutamide), the CAMKK2 inhibitor STO-609 (10uM) or the combination treatment for 72h (viable cell counts [trypan blue exclusion] using a Vicell cytometer, data expressed as % vehicle control). (b) Pharmacokinetic measurement of plasma concentrations of STO-609 in mice following IP or IV injection. STO-609 levels were measured using LC-MS/MS and quantified relative to standard curve measurements. (c) Images of xenograft tumour bioluminescence measured on weeks 1-5 from a single representative mouse from castrated mice were treated with the CAMKK2 inhibitor STO-609 (10 µmol/kg) or vehicle control (DMSO) three times per week and imaged once per week following IP injection of 150 mg/kg luciferin. (d) PFK activity measurements from C4-2B xenograft tumours treated with STO-609 or vehicle control (represented as mean +/- SEM). (e-h) H&E staining of normal mouse prostate sections from xenograft experiments to show the effects of castration and CAMKK2 inhibition on normal prostate histology (full indicates non-castrated and cast. indicates castrated mice; arrows indicate gland lumen).